Journal of Structural Geology, Vol. 14, No. 8/9, pp. 963 to 972, 1992
Printed in Great Britain

0191-8141/92 $05.00+0.00

Volume loss and deformation around conjugate fractures: comparison between a natural example and analogue experiments

F. ODONNE

Laboratoire de Géologie Structurale et Tectonophysique, and URA CNRS No 67, Université Paul-Sabatier, 38 rue des 36-ponts, 31400 Toulouse, France

and

G. MASSONNAT

Département Technique et Spécialité Gisement, ELF Aquitaine, Avenue Larribau, 64018 Pau Cédex, France

(*Received* 1 *October* 1991; *accepted in revised form* 2 *April* 1992)

Abstract—In well-stratified sedimentary rocks, measurement of the bedding offsets along fractures gives a value for the relative displacement at each location. To restore the undeformed geometry of the layers, the offset along each fracture must be cancelled. Restoration of the geometry enables the location of places where shortening is concentrated to be established, namely at the fracture intersection and at fracture tips. Slow displacement during deformation is demonstrated by the growth of fibres on the fault surfaces. Pressure solution inside the layers is responsible for the internal strain with associated volume loss. This mechanism is compatible with low strain rates giving aseismic displacements along the fractures. To model rock rheology dominated by pressure solution, a viscous material (paraffin wax) has been employed in the analogue model. Volume loss in nature is represented by area changes during the analogue experiments. In the experiments, shortening is concentrated around the fractures in exactly the same geometrical positions as in nature. When the amount of displacement is different on each of the two fractures, one of the fractures is observed to offset its conjugate fracture. When this is the case, relative timing of displacement along conjugate fractures cannot be determined without ambiguity from the observation of fracture offsets.

INTRODUCTION

THE idea that a fault is a kinematic discontinuity along which two rigid blocks move in opposite directions can sometimes lead to geometric incompatibilities. Ramsay & Huber (1987) describe an example of synchronous development of two conjugate faults where the displacement on fault surfaces leads to the development of voids. A sequential movement on the fractures avoids the development of such voids, which are not observed in natural examples. Nevertheless, contemporaneous movement along cross-cutting conjugate faults is possible (Horsfield 1980), and obviously refutes the initial assumption of rigid blocks.

The aim of this work is to describe an example of contemporaneous displacement on conjugate fractures. Two questions arise from the assumption of non-rigidity of the blocks moving along the fault surfaces. (i) How is compatibility maintained by strain in the adjacent blocks? (ii) How does the system move during the deformation?

A natural example provides part of the answer to the first question, but an analogue model is of great help in investigating the kinematic evolution of the system. These two examples are described and compared. The data provided by each example are summarized in the conclusion.

THE NATURAL EXAMPLE: DEFORMATION AROUND CONJUGATE FRACTURES

Near Saint-Jean-de-Luz, in the western Pyrenees, the shore cliffs provide numerous outcrops of Cretaceous Flysch. These very well-stratified sedimentary rocks exhibit some conjugate normal faults along which the horizontal layers are displaced (Fig. 1a). Fibres on the fractures indicate that the displacement lies within the plane of the figure. The fibres, which are made of calcite, also provide proof of post-sedimentary deformation, accommodated by aseismic displacement (Gratier & Gamond 1990). The displacement is greater on the right dipping fracture than on the conjugate left-dipping fracture (Fig. 1a), and this displacement is accommodated by bending of the fractures as shown by Freund (1974) and Gapais *et al.* (1991).

To restore the undeformed geometry in the plane of Fig. 1(a), each offset along the fractures must be cancelled on the line drawing of the natural example (Fig. 2). The piece of paper is cut along the lines of the fractures and the blocks are displaced to restore the unbroken shape of each layer before fracturing. In this example, the displacement of the layers cannot be totally cancelled without creating voids on the fracture surfaces (Fig. 3). As such voids have no physical reality, we must conclude some accommodation by deformation

and mass transfer around the fractures (Carrio-Schaffhauser & Chenevas-Paule 1989). The non-constant value of the offset along the fractures also indicates the occurrence of strain during the displacement. From a maximum value near the middle of the fracture, the relative displacement is reduced to zero at the fracture tips. This agrees with numerous observations of natural faults (Walsh & Watterson 1989).

From Fig. 1(a), it can be seen that the thickness of the layers is constant far from the fractures but is reduced in some places close to the fractures. By cutting the sheet of paper representing Fig. 2 along the fracture lines and inside some layers, it is possible to cancel the bedding offsets and restore the thickness of all the layers (Fig. 4). This restoration of the initial geometry shows that, during the deformation, the fracture with large relative displacement offsets its conjugate. It also shows that the thickness of the layers has been reduced around fracture tips and at the intersection of the conjugate fractures. If the assumption of no displacement perpendicular to the plane of the figure is correct, then the black spaces in the layers must represent an area change in the figure related to a volume loss during deformation. This volume change may be accommodated by two mechanisms: either density changes (porosity) or chemical composition changes (mass transfer). The first results show that porosity never exceeds 2% in flysch, and chemical analyses show the calcite concentration to be about 50%. Using the insoluble contents, I_p in protected zones (far from a fault) and I_e in exposed zones (close to a fault), the volume changes are calculated in three layers as $(I_p/I_e) - 1$ (Gratier 1983). In two layers, the volume loss reaches 15% close to the faults, but in the third no volume loss can be seen. Area changes between initial and restored geometry of the structure indicate volume changes during the deformation, because the displacement lies within the plane of the figure. In a few layers, veins of calcite indicate horizontal stretching. The restoration takes into account this stretching, but its effect is very small in relation to the complete deformation. Throughout the whole structure the volume loss is 2%, where the accuracy of the measurement is 0.3%. Thus, the system cannot be said to be completely closed at the scale of the structure (Gratier 1983). Therefore, taking account of volume loss during deformation and the occurrence of fibres on the fractures, indicating a slow displacement rate, it appears that pressure solution is the mechanism responsible for deformation around these fractures (Gratier & Gamond 1990) but not, of course, for the fracturing. Rispoli (1981) demonstrated that pressure solution could occur synchronously with relative displacement along a fracture. Pressure solution is known to occur during faulting (Carrio-Schaffhauser & Gaviglio 1990) and during large displacement along an existing fault surface (Odonne 1990).

By drawing a grid on Fig. 1(a) before cutting the sheet of paper to reconstruct the initial geometry, the displacement vector field can be drawn (Fig. 5). Two layers, the positions of which appear to be invariant, are used to mark the horizontal. On the same figure are drawn the fault traces in the deformed shape (continuous lines) and in the reconstructed initial shape (dotted lines). This figure shows that the upper and lower blocks converge while the two lateral blocks are extruded. It also shows rotation and bending of the longest fracture while the conjugate fracture is only offset.

In summary, this natural example shows the following.

(i) The relative displacement is not constant along each fracture.

(ii) The non-constant layer thickness indicates a volume loss during deformation.

(iii) The fibres on the fault surfaces grew during slow aseismic displacement.

(iv) The fracture on which relative displacement is larger offsets the conjugate fracture.

ANALOGUE EXPERIMENT

From the geometrical analysis of the natural example, the areas of maximum strain around the fractures can be located and the initial geometry of the structure restored. But this analysis does not supply any information about the timing of fracturing. The movement of the fractures during deformation is not completely known. To understand the possible evolution of conjugate fractures during deformation of a sedimentary multilayer by pressure solution, we use an analogue model.

On fracture surfaces, where the length of the fibres corresponds to about the offset values along the fractures, the fluid mechanism must have had a negligible effect on this offset value vs the pressure solution accommodation. All the slip on the fractures is accommodated by pressure solution, perhaps after Mohr–Coulomb slip at the first increment. Pressure solution requires a very long time (Rutter 1976) and the corresponding displacement rate is aseismic (Gratier & Gamond 1990). As a deformation that requires 10^6 years in nature is achieved in half an hour in the model, where time is acelerated by about 10^9, we have chosen to study, in this experiment, the accumulation of inelastic strain and the kinematics of the deformation, rather than the propagation of the fractures themselves.

The behaviour of rocks deforming by pressure solution is analogue to a linear viscous body (Laubscher 1975, Rutter 1976, Gratier 1987). A viscous material has therefore been selected for this experiment: paraffin wax with a melting point of 46–48°C, a viscous material with a non-linear viscosity (Mancktelow 1988), manufactured by Merck. At the temperature of the experiment, 30°C, the stress exponent n is about 1.8 (Fig. 6). We can expect that experimental deformation should be more heterogeneous than that occurring in the natural material.

The experiment

The models consist of a single layer of paraffin wax, 1.1 cm thick, deformed in a rectangular box, 70 × 60 cm,

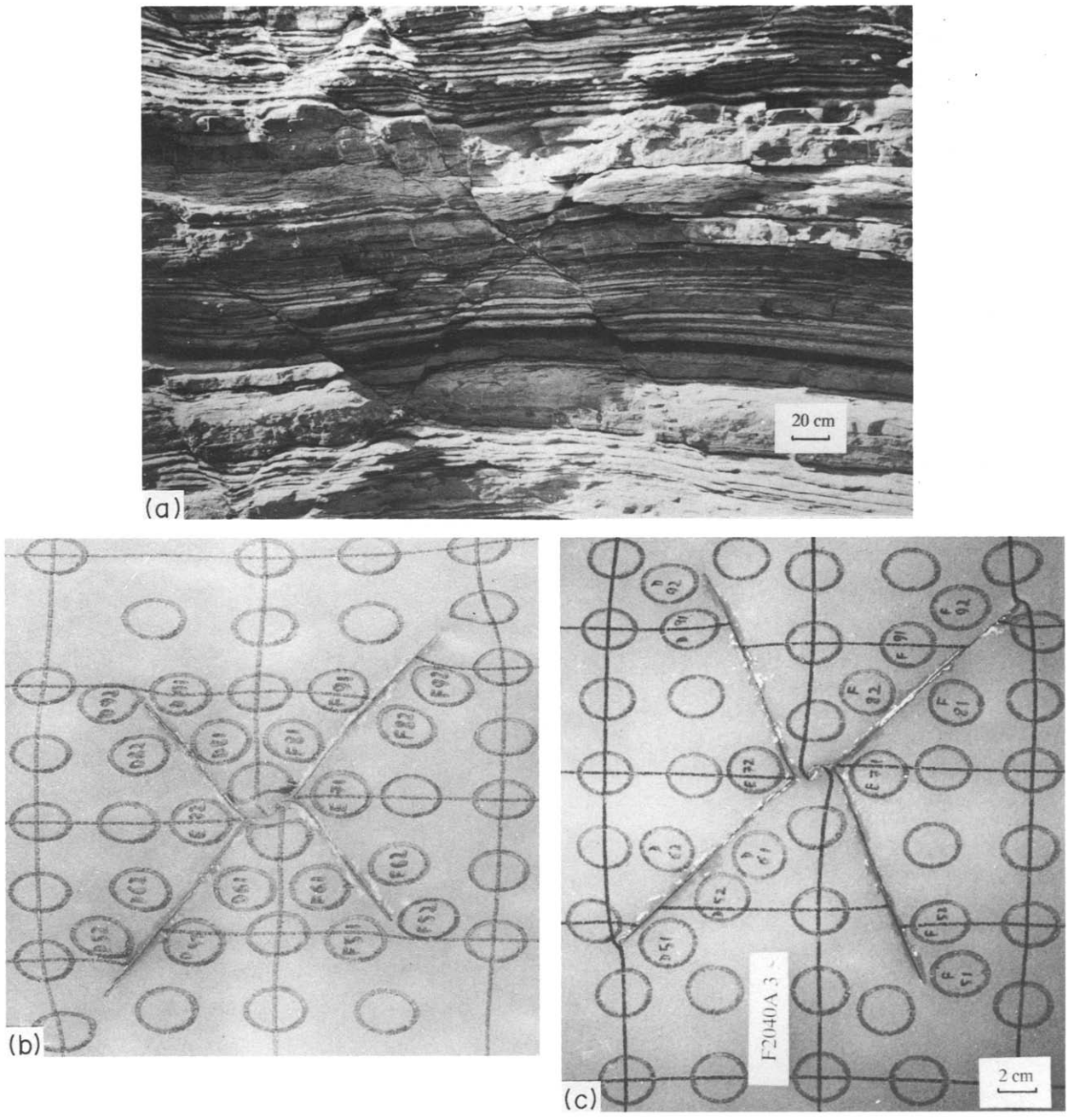

Fig. 1. (a) Conjugate fractures in the Cretaceous Flysch near Saint-Jean de Luz (French Pyrenees). The bedding offset indicates an important relative displacement along the right-dipping fracture. Fibres on the fracture surfaces imply a slow displacement rate. (b) & (c) Top views of the analogue experiment. The conjugate fractures have been cut in the paraffin layers before deformation. Small circles indicate the strain at each place on the surface of the models. Compression was applied at the top of the figures. The models have unequal original fracture length (b) or unequal orientation of the fractures relative to the compression direction (c).

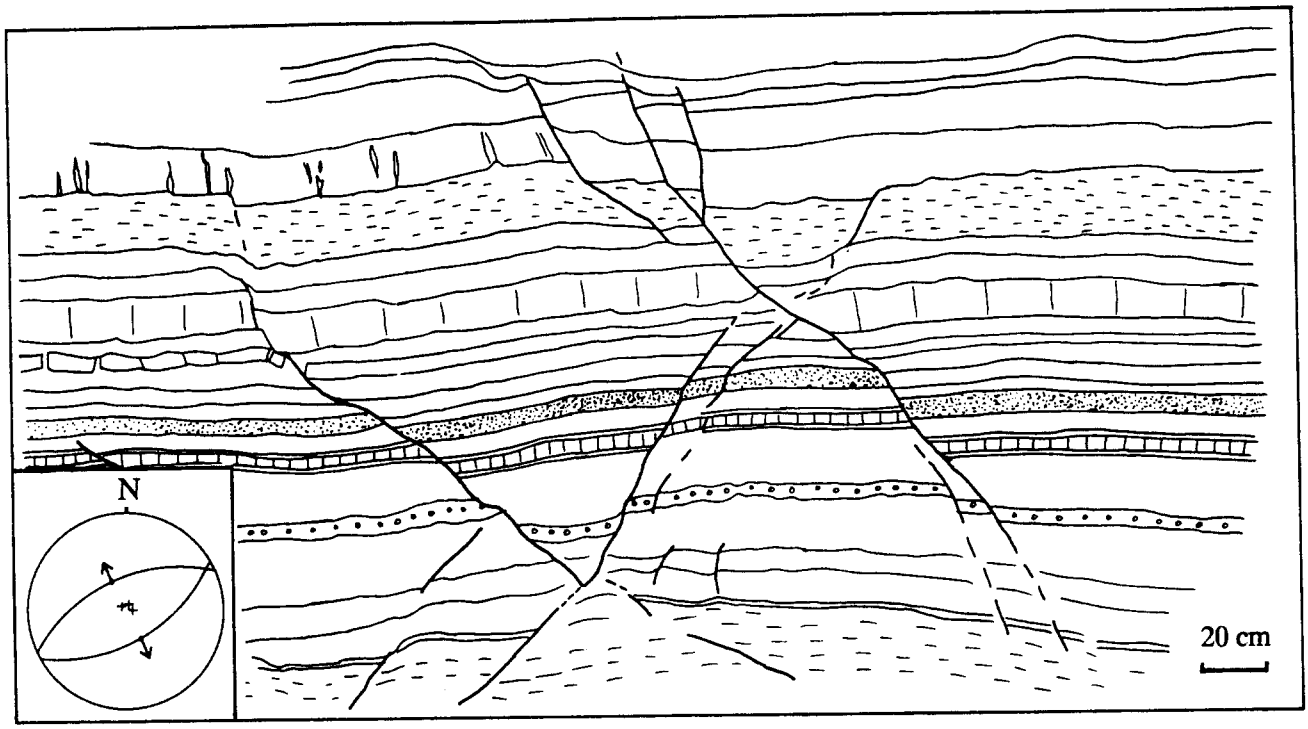

Fig. 2. Line drawing of the layers and the conjugate fractures from Fig. 1(a). The bending of the fault surfaces is clear. Note also the non-constant thickness of some layers. The small stereogram shows the positions of bedding (crosses), fracture planes and fibres (arrows).

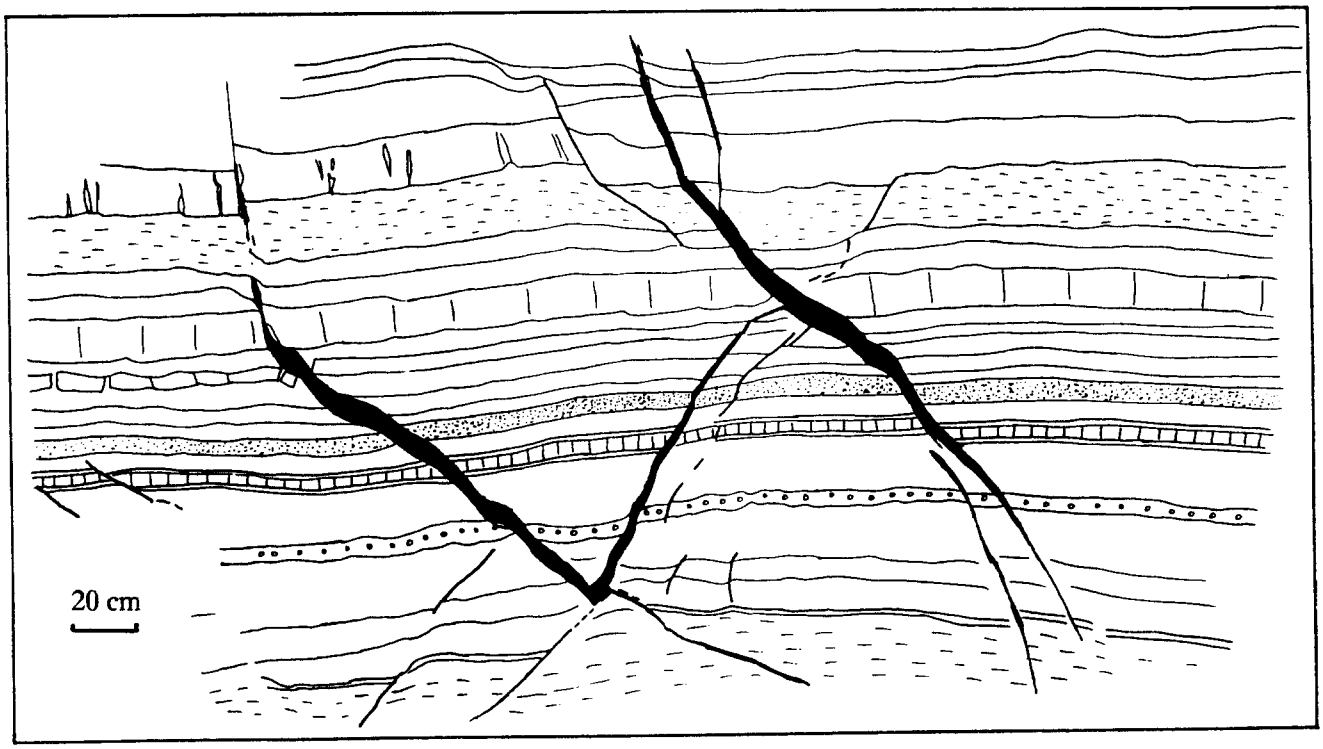

Fig. 3. To restore the undeformed geometry of Fig. 2, rigid blocks are displaced to cancel the beddding offset. The result shows that restoration is impossible without creating voids along fracture surfaces (black).

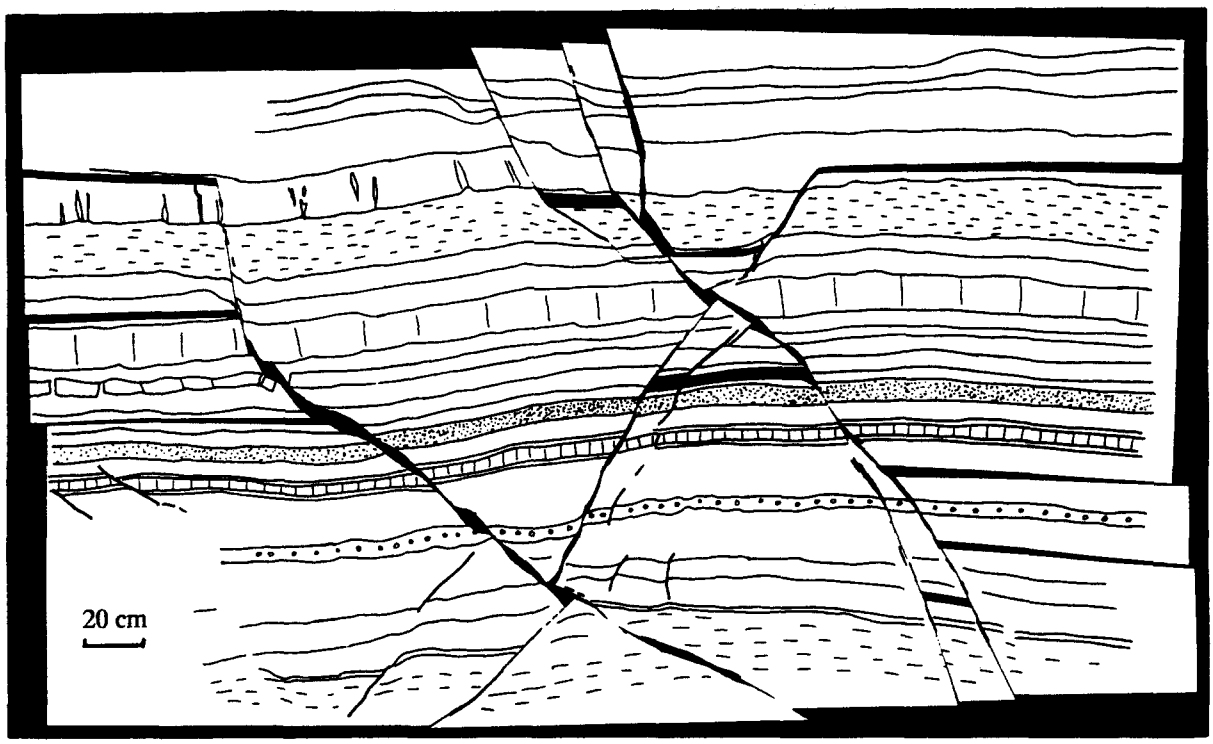

Fig. 4. When internal strain in the layers is also considered, the bedding offset can be cancelled along the length of the fractures. The thickness of each layer is restored graphically. This restoration leads to the development of voids in some layers. These voids represent that part of the layer which has been removed by pressure solution. The major part of the volume loss is concentrated at fracture tips and at the fracture intersection.

by moving one of the shorter sides at a controlled rate of displacement. The layer of paraffin is smaller than the box, 70 × 45 cm, and when the model is subjected to compression the sides are free to expand. At the bottom of the box, friction is reduced by Silicone grease (Rhone-Poulenc, 70428) and silicone oil (Rhodorsil, 47 V 300) added in the proportion of three parts of grease to one part of oil. At 30°C, the viscosities of the materials are 3×10^5 Pa s for the paraffin wax and 10 Pa s for the grease. To represent the conjugate fractures, two slits were made in the paraffin before deformation and filled with grease to allow relative displacement. The deformation of small circles, drawn on the free surface of the layer (Figs. 1b & c), indicates the amount of strain at each point on the surface of the model. As the displacement of the wall is stopped every 5 cm, for strain measurement, the strain history can be inferred from the deformation at successive stages.

The offset of a fracture by its conjugate is observed in the natural example. The experiment allows the possibility to investigate if this offset occurs systematically or if specific geometrical conditions are required. In order to consider this question, three types of experiments were prepared. In the first, the conjugate fractures were absolutely symmetrical. The two fractures were orientated at 30° to the compression direction, which were of the same length (30 cm) and which cross-cut each other in the middle of the model. The main result of this experiment is that the system remains symmetrical during the deformation, and that neither fracture is displaced by its conjugate. To introduce asymmetry into the system, it is possible to change either the orientation or the length of the fractures. Both possibilities were investigated. The results of these two experiments are consistent: (i) where the fractures are of unequal length, the longer fracture offsets the shorter one (Fig. 1b), because the displacement in the middle of the fracture is a function of the length of the fracture (Walsh & Watterson 1989); (ii) where the orientation of the fractures is not symmetrical to the compression direction, one of the fractures offsets its conjugate (Fig. 1c). The orientation of the fractures was changed by rotating the two fractures by 10°. One of the fractures is then orientated at 20° to the compression direction and the other at 40°. As the shearing stress is greatest on the second fracture, the relative displacement is largest along this fracture and offset of the conjugate occurs.

The first results of the experiments is therefore that an asymmetry must be introduced into the system in order to create the offset of a fracture by its conjugate. Unequal length of the two fractures or unequal orientation relative to the compression direction can produce the same result. As the reason for the offset in the natural example is not established beyond doubt, the two experiments should be presented. But, as they produce very similar results, only the experiments with fractures of unequal length (Fig. 1b) will be fully analysed. At the end of the experiment, the longest fracture with a left-lateral movement offsets the conjugate. The trace of this longest fracture is still not straight; it is itself slightly offset by the conjugate, or bent during the deformation as in the natural example.

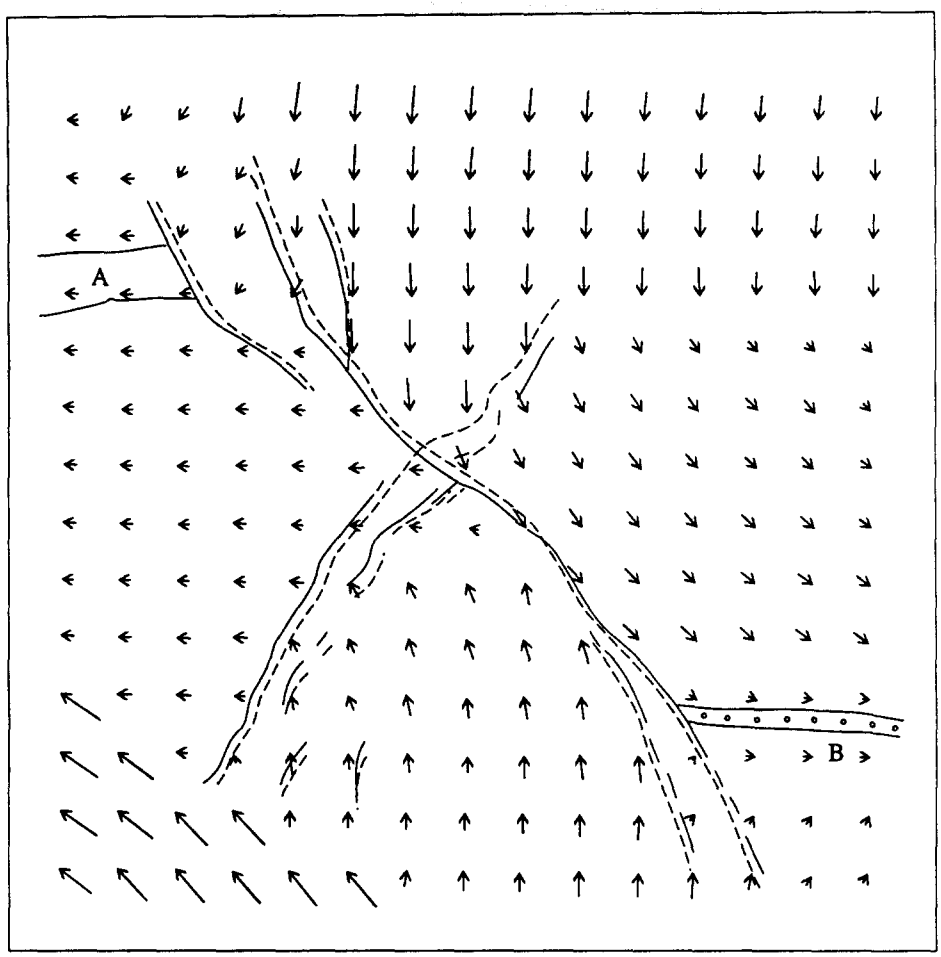

Fig. 5. Displacement vector field for the natural example. A grid drawn on Fig. 2 gives the final positions of the vectors. The same grid after restoration of the initial geometry gives the initial positions of the vectors. Two layers (A and B), the positions of which appear to be invariant, are used to mark the horizontal. The upper and lower blocks converge while the two lateral blocks are extruded. The final positions (continuous lines) and the reconstructed initial position (dotted lines) of fault traces are also drawn on the figure. The longest fracture is rotated and bent, while the conjugate is only offset.

Strain analysis

Displacement vectors relative to the centre of the model exhibit the particle displacement paths during the deformation. The vectors show that the displacements are very different in the four domains delimited by the fractures. The two lateral domains, in the obtuse angle of the fractures, are extruded while the other two domains converge (Fig. 7). Compare with Fig. 5 of the natural example.

As the top surface of the model is free, the model thickens during the deformation. Every change in the

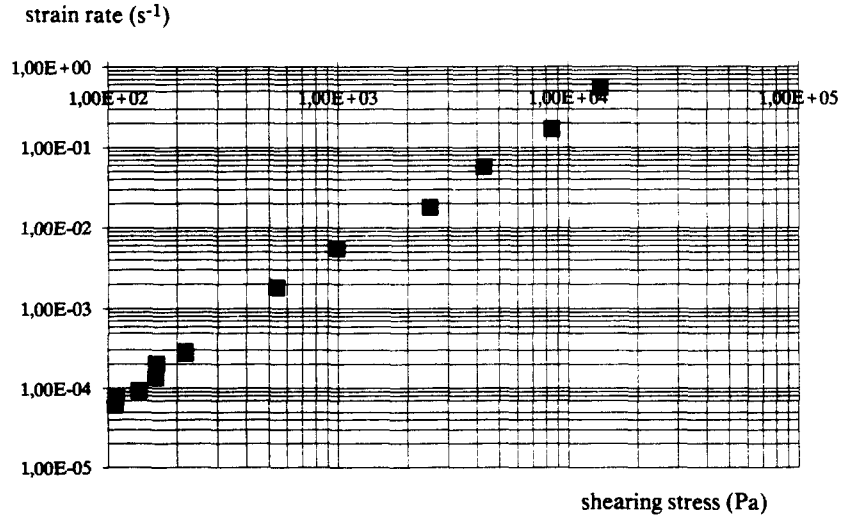

Fig. 6. Strain rate vs shearing stress curve of the 46–48°C paraffin Merck on a log–log diagram. The stress exponent is about 1.8.

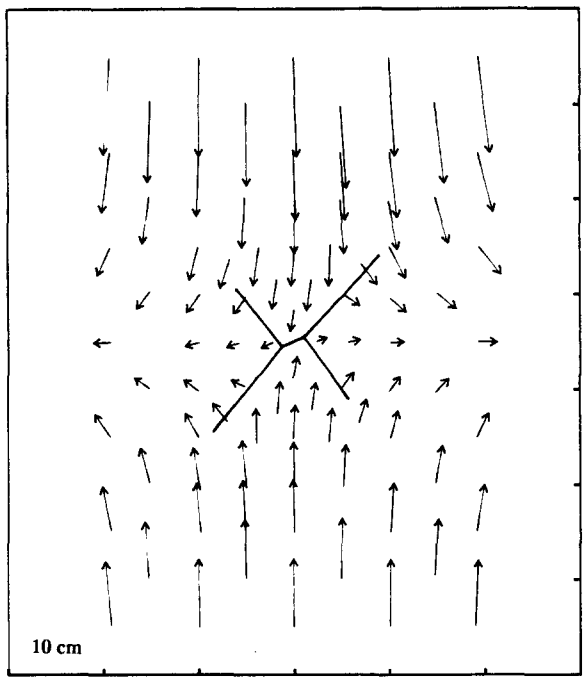

Fig. 7. Displacement vectors relative to the centre of the model. Two domains have moved apart while the other two domains converged.

thickness of the layer is balanced by a change in the area of the ellipses. The position and shape of each ellipse is measured throughout the experiment, and a computer program used to compare the data and indicate where the thickness of the model changes (Fig. 8). The ellipses are represented by small squares; where the increase in thickness of the layer exceeds 25%, two large concentric squares are drawn. The area change at the surface of the layer is concentrated near the moving wall but also at the fracture intersection and at the fracture tips. Further from the moving wall, only the longest fracture is able to produce an important area change, because there is considerable relative displacement along this fracture. The conjugate fracture, where relative displacement is small, is unable to induce the same concentration of strain.

A unilateral compression acts on the model, the displacement of which is reduced by the friction on the base plate, so the strain is greater close to the moving wall (Fig. 8). We have to eliminate this part of the strain, which is superimposed on the heterogeneous strain introduced by the fractures. All ellipses located at equal distances from the moving wall are compared. A mean value of the length of short axes of finite strain ellipses in each group is calculated, then each ellipse is checked with the mean of this group. If the shortening differs by more than 10% from the mean, the size of the small hexagons that represent the ellipses is changed. Two large concentric hexagons are drawn if the shortening is greater than the mean, and a large dotted hexagon if less (Fig. 9). The shortening is concentrated at fracture tips in the extruded domains, especially at the tips of the longest fracture, and at fracture intersection in the domains that intrude, but most of the blocks that converge are protected domains. The location of shortening at the fracture intersection and at fracture tips corre-

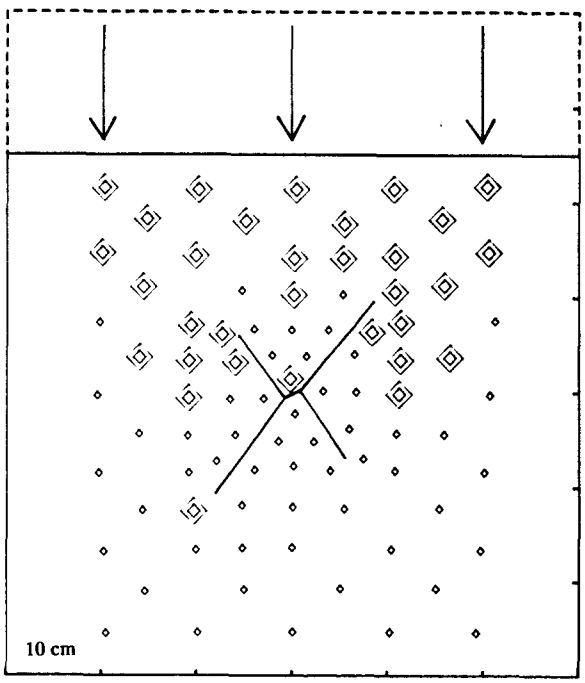

Fig. 8. Thickening of the model during the experiment. Where the thickening reaches 25%, two large concentric squares are drawn. Small squares represent the ellipses without area change. The area changes are concentrated near the moving wall and at the fracture intersection and fracture tips, except at the tip of the conjugate fracture, which is located far from the moving wall. The small relative displacement on this fracture does not lead to an important concentration of strain.

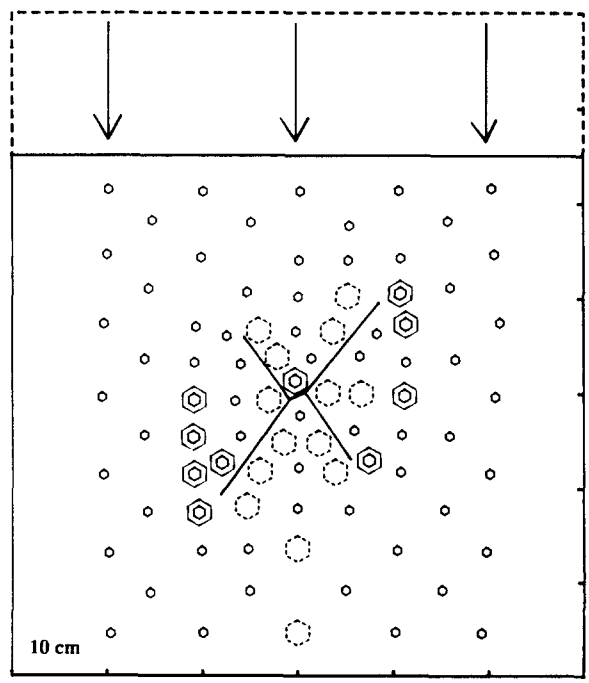

Fig. 9. Comparison of strains at equal distances from the moving wall, to eliminate strain heterogeneity associated with the wall and friction on the base plate. Horizontal shortening more that 10% greater than the mean is represented by large concentric hexagons, more than 10% less than the mean is represented by dotted hexagons. Shortening appears to be concentrated at fault tips and at the fracture intersection.

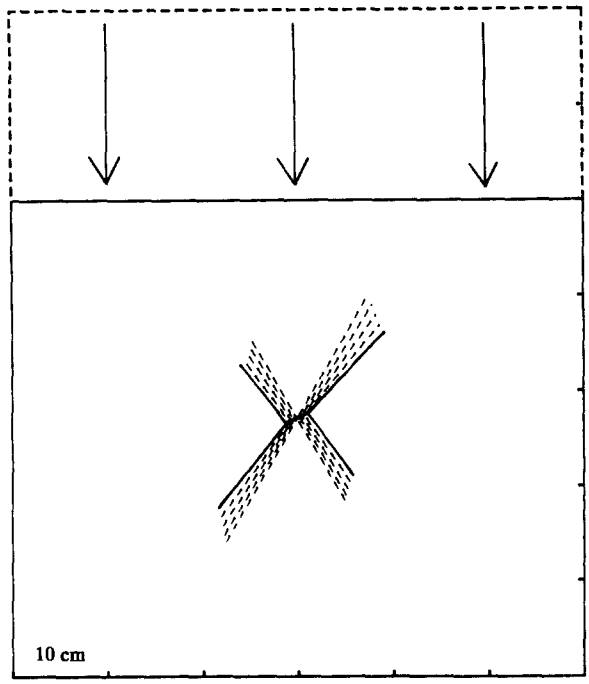

Fig. 10. Successive positions of the fractures during deformation. The positions of the fractures at successive stages of the experiment are superimposed on the final positions of the fractures. The translation has been removed graphically so that the rotation and offset appear clearly. The longest fracture rotates, while the short fracture is offset by its conjugate and is rotated less.

sponds to areas of volume loss in the natural example (Fig. 4).

The rotation of the fractures during the deformation is clear (Fig. 10). This figure shows the superimposition on the final positions of the fractures, of all successive positions during previous stages of deformation. The general translation that occurs during the experiment has been removed graphically from this figure. The longest fracture appears to rotate, whereas the rotation of the conjugate fracture is small; the conjugate fracture is mainly offset and displaced by the longest fracture. Compare with Fig. 5.

In summary, the analogue experiment shows the following.

(i) The two domains in the obtuse angle of the fractures are extruded while the domains facing the compression collide with each other.

(ii) The offset of a fracture by its conjugate requires an asymmetry in the disposition of the fractures. This asymmetry is provided by unequal lengths or unequal orientations of the fractures.

(iii) The fracture on which the relative displacement is largest rotates while the conjugate is displaced and rotates very little.

(iv) Area change and deformation are located at the fracture intersection and at fracture tips.

CONCLUSION

Comparison of the natural example with the analogue model shows a great number of similarities. The viscous behaviour of the analogue material provides analogy with the natural example. Geometric patterns of strain, due to volume loss during a natural deformation, can be modelled by area change during an analogue experiment in non-plane strain. The results from the model are consistent with natural data and, moreover, they provide original data on the kinematic evolution of the system. The model shows that during deformation the two blocks are moved apart perpendicularly to the compression direction. Corresponding horizontal displacements in the natural example are not so clearly recorded, because displacement markers, provided by the stratification, indicate vertical displacements only. A synchronous displacement on conjugate fractures is possible if the blocks adjacent to the fractures are not absolutely rigid. The distribution of strain is not homogeneous in the blocks: shortening is concentrated at fracture tips and at the fracture intersection. On the fracture surfaces, fibres are proof of seismic displacement. This is further supported by the occurrence of pressure solution as a deformation mechanism in the layers. The offset of a fracture by its conjugate requires an asymmetry in the system. This asymmetry can be introduced by an unequal orientation of the fractures relative to the compression direction or by an unequal original length of the fractures. In this case, the offset of a fracture by its conjugate is not necessarily a criterion to determine the relative chronology for fracturing. The fracture on which the relative displacement is largest rotates during the deformation, while its conjugate is displaced without significant rotation.

Acknowledgements—We should like to thank J. Deramond and H. Koziol for their assistance in preparation of the manuscript. We thank B. Moine for his help with the chemical analysis. We are also grateful to J.-P. Gratier and N. Mancktelow for their careful reviews, which enabled us to improve this paper substantially, and to J.-P. Petit for many useful comments. Much of this work was carried out under Elf Aquitaine contracts.

REFERENCES

Carrio-Schaffhauser, E. & Chenevas-Paule, F. 1989. Quantification géométrique de la dissolution-cristallisation liée à une déformation cassante. *Bull. Soc geol. Fr.* **8**, 597–604.

Carrio-Schaffhauser, E. & Gaviglio, P. 1990. Pressure solution and cementation stimulated by faulting in limestones. *J. Struct. Geol.* **12**, 987–994.

Freund, R. 1974. Kinematics of transform and transcurrent faults. *Tectonophysics* **21**, 93–134.

Gapais, D., Fiquet, G. & Cobbold, P. R. 1991. Slip system domains, 3. New insights in fault kinematics from plane-strain sandbox experiments. *Tectonophysics* **188**, 143–157.

Gratier, J.-P. 1983. Estimation of volume changes by comparative chemical analyses in heterogeneously deformed rocks (folds with mass transfer). *J. Struct. Geol.* **5**, 329–339.

Gratier, J.-P. 1987. Pressure solution-deposition creep and associated tectonic differentiation in sedimentary rocks. In: *Deformation of Sediments and Sedimentary Rocks* (edited by Jones, M. E. & Preston, R. M. F.). *Spec. Publs geol. Soc. Lond.* **29**, 25–38.

Gratier, J.-P. & Gamond, J. F. 1990. Transition between seismic and aseismic deformation in the upper crust. In: *Deformation Mechanisms, Rheology and Tectonics* (edited by Knipe, R. J. & Rutter, E. H.). *Spec. Publs geol. Soc. Lond.* **54**, 461–473.

Horsfield, W. T. 1980. Contemporaneous movement along crossing conjugate normal faults. *J. Struct. Geol.* **2**, 305–310.

Laubscher, H. P. 1975. Viscous components in Jura folding. *Tectonophysics* **27**, 239–254.

Mancktelow, N. S. 1988. The rheology of paraffin wax and its usefulness as an analogue for rocks. *Bull. geol. Inst. Univ. Uppsala* **14**, 181–193.

Odonne, F. 1990. The control of deformation intensity around a fault: natural and experimental examples. *J. Struct. Geol.* **12**, 911–921.

Ramsay, J. G. & Huber, M. I. 1987. *The Techniques of Modern Structural Geology, Volume* 2: *Folds and Fractures*. Academic Press, London.

Rispoli, R. 1981. Stress fields about strike-slip faults inferred from stylolites and tension gashes. *Tectonophysics* **75**, T29–T36.

Rutter, E. H. 1976. The kinetics of rock deformation by pressure solution. *Phil. Trans. R. Soc. Lond.* **A283**, 43–54.

Walsh, J. J. & Watterson, J. 1989. Displacement gradients on fault surfaces. *J. Struct. Geol.* **11**, 307–316.